IL NUOVO CIMENTO Vol. 35 C, N. 4 Luglio-Agosto 2012
DOI 10.1393/ncc/i2012-11265-x

Colloquia: PAVI11

Two-photon exchange and normal spin asymmetries in the A4 experiment

D. Balaguer Ríos
Institut für Kernphysik - Mainz, Germany

ricevuto il 13 Ottobre 2011; approvato il 5 Maggio 2012
pubblicato online il 25 Giugno 2012

Summary. — The A4 Collaboration at the MAMI facility has measured, at backward angles and at $Q^2 = 0.23\,(\mathrm{GeV}/c)^2$ and $Q^2 = 0.35\,(\mathrm{GeV}/c)^2$, the asymmetry in the elastic and quasielastic scattering of normally polarized electrons on hydrogen and deuterium, respectively. Some preliminary results will be presented.

PACS 13.60.Fz – Elastic and Compton scattering.
PACS 11.30.Er – Charge conjugation, parity, time reversal, and other discrete symmetries.
PACS 13.40.Gp – Electromagnetic form factors.

1. – Introduction

The two-photon exchange amplitude in the elastic-nucleon scattering can explain the discrepancy between the Rosenbluth technique and the Polarization transfer method in the measurement of proton form factors [1]. The beam normal spin asymmetry (BNSA) in the elastic scattering of nomal polarized electrons off unpolarized nucleons is sensitive to the imaginary part of this amplitude.

A model calculation of the imaginary part of the two-photon exchange amplitude includes all the intermediate hadronic states, the ground state of the nucleon and the excited hadronic π-N states, whose transition amplitudes are evaluated with the Mainz unitary isobar model for pion photo- and electroprodution on the nucleon, called MAID.

The BNSA is of the order of 10^{-5} and it is azimuthally modulated by $\cos\phi$. The A4 experiment, able to measure asymmetries of the order of 10^{-6}, suits to measure the BNSA and to observe the azimuthal modulation thanks to the high symmetry of the detector.

2. – Experimental set-up

In the A4 experiment at the MAMI facility a polarized electron beam hits an unpolarized target of either liquid H_2 or D_2. An electromagnetic calorimeter counts the

elastically (quasielastically) scattered events and allows the measurement of their energy with an energy resolution of $\Delta E/E = 3.9\%/\sqrt{E(\mathrm{GeV})}$. The elastic scattered electrons are therefore energetically separated from the inelastic scattered ones.

The detector operates at backward angles covering the scattering angle 140°–150°. It covers also the whole azimuthal angle symmetrically around the beam line.

At backward angles an extra detector of plastic scintillators before the calorimeter distinguish charged and neutral particles, since the amount of background of gamma photons from the π^0 decay is high and it would hide the elastic peak.

The asymmetry is $A_\perp = (N^+ - N^-)/(N^+ + N^-)$, where $N^\pm$ is the number of the elastic (quasielastic) events for each polarization state. For more details see [2].

For a more detailed description of the actual experimental setup of A4 see [3].

3. – Data analysis

Every run of 5 minutes four energy spectra histograms are generated: two of charged particles and two of neutral particles, for each polarization state.

The elastic (quasielastic) peak is separated in the spectrum of charged particles, where still a neutral background arises from the conversion of photons in the materials before the scintillators. The energy spectrum has been understood using a Monte Carlo simulation [4].

We use a method to estimate the background pollution and its own BNSA from the experimentally observed spectrum of charged particles. This method uses two parameters: a shift δ, related to the loss of energy of the electrons in the scintillators, and a scaling factor ϵ, related to the conversion probability of the gamma photons. For details see [4].

The asymmetry is extracted from the histogram of charged particles A_e applying cuts to delimit the elastic peak. Then it is corrected from the asymmetry of the background A_γ, $A_\perp^{ph} = (A_e - fA_\gamma)/(1-f)$, where f is the fraction of background in the elastic (quasielastic) peak.

Several systematic corrections are applied to the extracted raw asymmetry: normalization to the fluctuations of the luminosity signal, including the correction of the non-linearity of this signal; subtraction of the false asymmetries due to the helicity correlated differences in the beam parameters; contribution of the quasielastic events on the aluminium windows, which have their own asymmetry; deviation of the electron spin direction, and normalization to the electron beam polarization.

The systematic error is calculated for every systematic correction mentioned above and additionally the error of the background subtraction, the propagation of the uncertainties of the scaling-shift model to the BNSA and the smearing in the asymmetry distribution due to the non-helicity correlated fluctuations of the beam parameters.

4. – Preliminary results

In fig. 1 one can see the azimuthal modulation of the raw asymmetry at $Q^2 = 0.23$ $(\mathrm{GeV}/c)^2$ (corresponding to the beam energy 315 MeV) with H_2 (left) and D_2 (right) as target, while in fig. 2 one can see this dependence of the extracted BNSA at $Q^2 = 0.35\,(\mathrm{GeV}/c)^2$ (corresponding to 420 MeV). The $\cos\phi$ dependence is clearly observed.

The applied systematic corrections and the error budget of the BNSA at $Q^2 = 0.23$ for both targets employed can be read in table I.

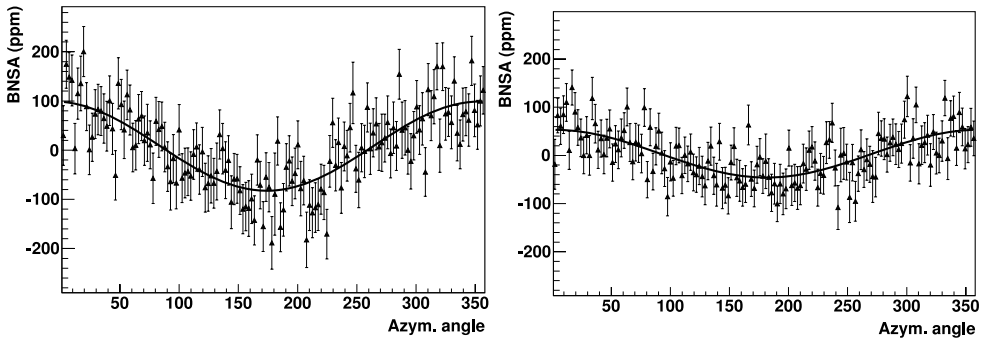

Fig. 1. – Left: azimuthal dependence of the BNSA for H_2 (elastic scattering). Right: azimuthal dependence of the BNSA for D_2 (quasielastic scattering), both at $Q^2 = 0.23\,(\mathrm{GeV}/c)^2$.

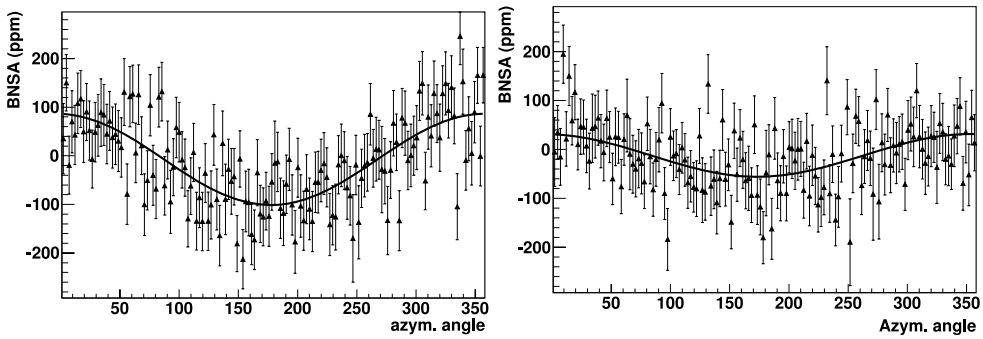

Fig. 2. – Left: azimuthal dependence of the BNSA for H_2. Right: azimuthal dependence of the BNSA for D_2, both at $Q^2 = 0.35\,(\mathrm{GeV}/c)^2$.

TABLE I. – *Systematic corrections and error budget for the measurements at* $Q^2 = 0.23$ *and target* H_2 *(left) and* D_2 *(right).*

	Scaling factor	Error(ppm)	Scaling factor	Error(ppm)
Polarization	0.77	3.29	0.79	2.23
	Correction(ppm)	Error(ppm)	Correction(ppm)	Error(ppm)
Dilution of γ backgr.	−1.10	1.16	2.73	1.28
ϵ, δ param.	–	2.90	–	0.97
Helicity corr. beam diff.	−0.12	0.70	−0.40	0.32
Non-helicity corr.beam fluc.	–	1.03	–	1.14
Al windows	−1.93	0.10	0.50	0.05
Random coinc. events	−1.25	0.07	−1.55	0.10
Luminosity	−0.61	0.20	−0.97	0.41
Nonlinearity of L	−0.47	0.17	−0.82	0.25
spin angle deviation	−0.65	0.89	−0.90	1.30
Sum syst. errors		4.79		3.29

TABLE II. – *BNSA at backward angles. Above the measurements on proton and deuterium. Below the calculated BNSA on neutron using the static approximation.*

E (MeV)	Target	BNSA	Q^2 (GeV/c)^2
315	H_2	$(-96.61 \pm 4.13 \pm 4.79)$ pm	0.23
315	D_2	$(-55.46 \pm 3.04 \pm 3.29)$ pm	0.23
420	H_2	$(-97.42 \pm 4.73 \pm 5.11)$ pm	0.35
420	D_2	$(-49.97 \pm 4.20 \pm 2.18)$ pm	0.35
315	n	(40.00 ± 20.79) pm	0.23
420	n	(54.94 ± 22.11) pm	0.35

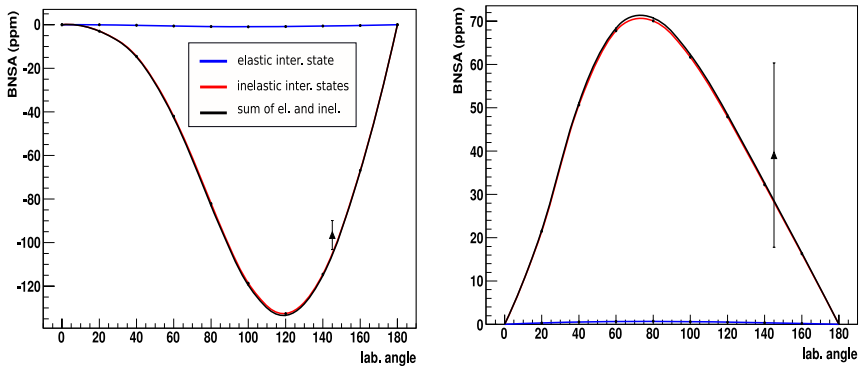

Fig. 3. – Model calculated BNSA as a function of the lab. scattering angle at 420 MeV of beam energy taken from [5], corresponding to scattering on proton (left) and scattering on neutron (right). The elastic (blue) and inelastic (red) contributions of the intermediate states to the BNSA are distinguished. The sum is in black. The preliminary A4 data points are shown at $\theta = 145°$.

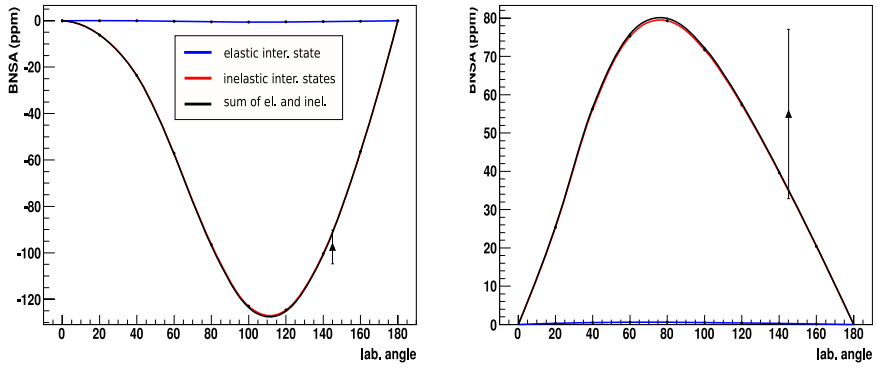

Fig. 4. – Model calculated BNSA as a function of the lab. scattering angle at 420 MeV of beam energy taken from [5], correponding to scattering on proton (left) and scattering on neutron (right). The elastic (blue) and inelastic (red) contributions of the intermediate states to the BNSA are distinguished. The sum is in black. The preliminary A4 data points are shown at $\theta = 145°$.

The preliminary results of the BNSA for the elastic scattering on H_2 and the quasielastic scattering on D_2 at $Q^2 = 0.23\,(\mathrm{GeV}/c)^2$ and $Q^2 = 0.35\,(\mathrm{GeV}/c)^2$ are presented in table II with both statistical and systematic errors.

In figs. 3 and 4 we can see the comparison of the measurement of the BNSA on proton with the model calculation. The calculation details the elastic contribution of the intermediate ground state of the nucleon and the inelastic one of the intermediate excited states, together with the sum.

The BNSA on neutron can be extracted from the BNSA on proton and that on deuterium using the static approximation:

$$A_\perp^d = \frac{\sigma_p A_\perp^p + \sigma_n A_\perp^n}{\sigma_p + \sigma_n}\,.$$

The calculated asymmetries on neutron and their propagated error are in table II, below. They present a high relative error due to the subtraction implied by the static approximation and the fact that the cross section on neutron is about 2 smaller than the cross section on proton at this kinematics. In figs. 3 and 4 the calculated BNSA on neutron are compared with the model calculations.

5. – Conclusion

We observe an excellent agreement of the measured BNSA on proton with the model calculation performed by [5]. The BNSA on the neutron, calculated using the static approximation, is also compatible with the model expectation for the neutron, figs. 3 and 4. In this model the excited intermediate hadronic states constribute substantially to the imaginary part of the two photon exchange amplitude.

6. – Outlook

More data has been taken at A4 with the detector operating at forward angles 30°–40° at different beam energies. Its analysis is in progress.

It is planned to take data with normal polarization of the electron beam at backward angles at the beam energy 210 MeV, that is at $Q^2 = 0.10$.

* * *

This work is supported by the Deutsche Forschungsgemeinschaft in the framework of the SFB 443. It is part of a PhD thesis.

REFERENCES

[1] Arrington J., *Phys. Rev. C*, **69** (2003) 022201.
[2] Maas F. E. *et al.*, *Phys. Rev. Lett.*, **94** (2004) 082001.
[3] Baunack S. *et al.*, *Phys. Rev. Lett.*, **102** (2009) 151803.
[4] Capozza L., PAVI9 Bar Harbor, 2009.
[5] Pasquini B. and Vanderhaeghen M., *Phys. Rev. C*, **70** (2004) 045206.